Dynamical Modeling with Inferred Cloud Distributions on Kepler-7b

mtroman@umich.edu

Mike Roman & Emily Rauscher

Department of Astronomy, University of Michigan

1. Summary: We run dynamical models of Kepler-7b with varying prescribed cloud distributions, based on the observed optical phase curves. We highlight differences in winds, temperatures, and model infrared phase curves.

2. Background:

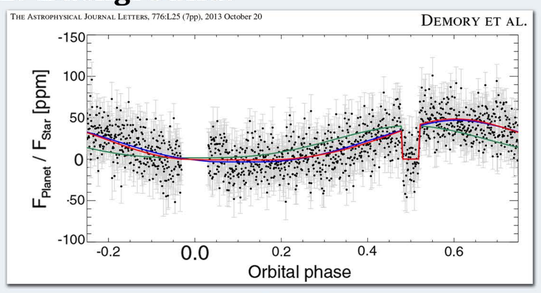

Visible phase curves of Kepler-7b show an asymmetry in the hot Jupiter's reflected light as a function of orbital phase. This has been interpreted as evidence of reflective clouds located west from the substellar point, consistent with the idea that clouds may be advected from the cooler night side to the warmer dayside by strong winds (Demory et al., 2012).

How do these reflective clouds affect the expected winds that carry them, as predicted by general circulation models (GCM)? Is this theory self-consistent?

Scattering calculations of Muñoz and Isaak (2015) provide constraints on the possible cloud distributions and scattering properties.

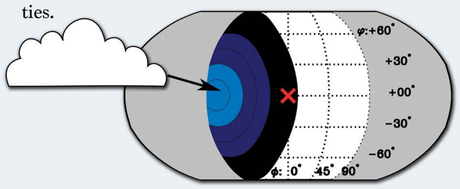

These provide four degenerate solutions with slightly different optical thicknesses, spherical albedos, and horizontal coverage. Here we focus on the first of these solutions, comparing them to corresponding models without clouds. We then compare the four to each other.

3. Modeling

We use an intermediate complexity GCM with a spectral dynamical core and double-gray radiative transfer, as previously employed by Rauscher & Menou (2012). The model was modified to include the effects of atmospheric scattering in the visible band, following the scheme of Toon et al (1989). Simulations were run at a spectral model resolution equivalent to a 48 X 96 lat/lon grid with thirty vertical layers.

Cloud vertical distributions are not strongly constrained by observations, so we will investigate different cloud heights, starting with a cloud peaking in optical thickness at ~100mb.

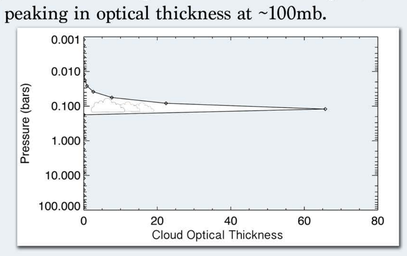

{Above} Assumed vertical profile of the cloud optical thickness for the center of the prescribed cloudy region in our first case. The profile shape is used for all locations, but the magnitude decrease with distance from the center of mapped region following Muñoz and Isaak (2015).

4. Preliminary Results:

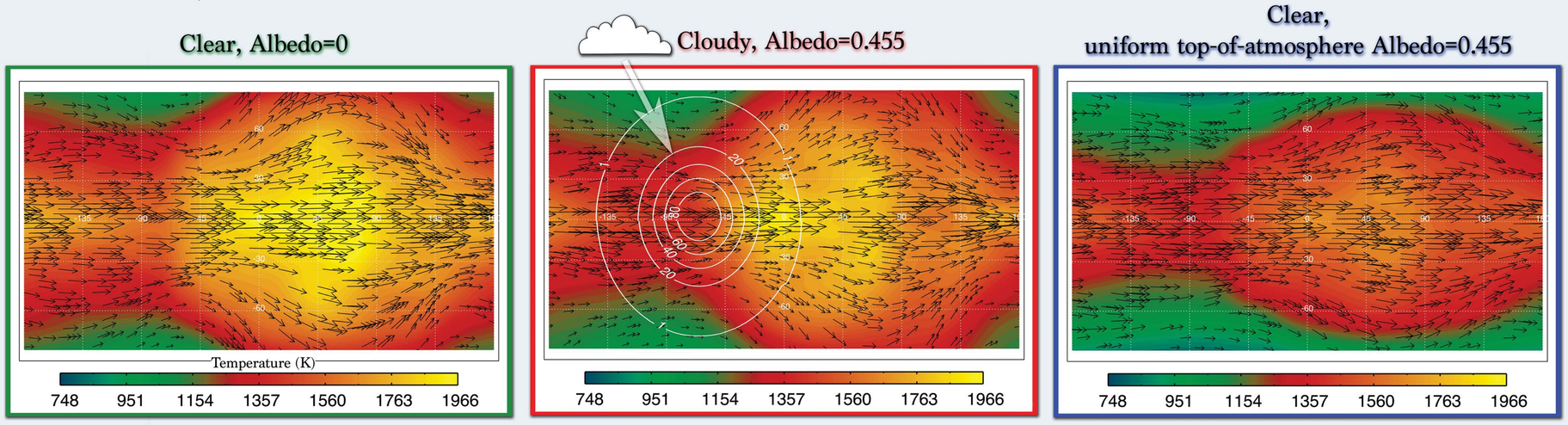

{Above} Simulated temperature field (color bar, K) and wind vectors at the infrared photosphere (~40mb) of Kepler-7b, for three different assumed cases:
(Left) Clear with visible albedo of zero; *(Center)* Cloudy with effective spherical albedo of 0.455 and total integrated optical depth of aerosols contoured in white; *(Right)* No aerosols, but with an artificial top-of-the-atmosphere albedo of 0.455, equivalent to the albedo of the cloudy case.

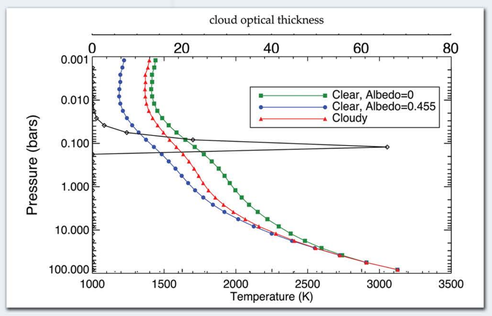

Global mean temperature profiles for each case, with maximum cloud vertical distribution included. Cooling becomes more prominent below the inhomogeneous cloud deck case (red) relative to the clear cases. The uniform reduced albedo case is still coolest.

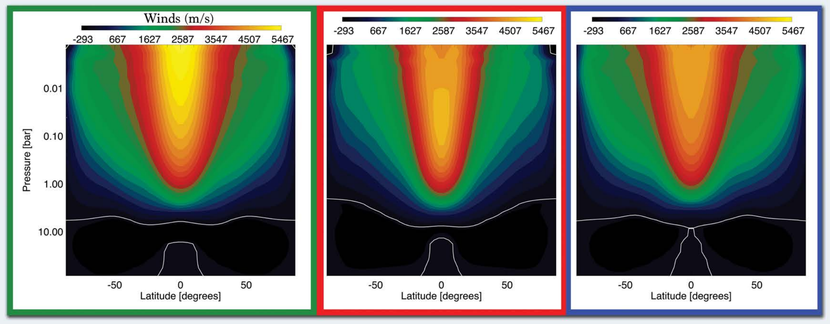

For the cases above, the zonal winds (m/s; easterly>0). The clear, zero albedo case shows the greatest wind speeds, peaking above 10mb; the cloudy case has reduced winds peaking at greater depths; the reduced albedo case is similar to the first clear case, but with lesser magnitude winds.

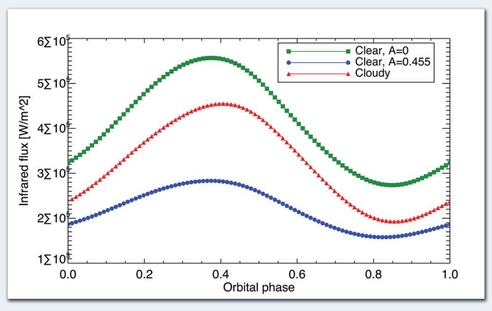

Modeled infrared phase curves for each case. The aerosol free atmospheres have maximum infrared emission at 44° sub-observer longitude resulting in peak fluxes at smaller orbital phase angles than the cloudy case; maximum emission for the cloudy case occurs at 32° longitude.

{Below} All four degenerate cloud distribution models of Muñoz and Isaak (2015) are compared. Plotted as before, prescribed model A has the lowest maximum integrated optical thickness (τ~100) with smallest sub-stellar offset; Prescribed model D has the greatest optical thickness (τ~200), though with greatest shift towards the western night side. *(Left)* The resulting temperature and wind fields at the IR photosphere are very similar, though model D shows the hottest dayside temperatures. With our assumed vertical distribution of clouds, we find model A results yields the coolest mean global temperature profiles just below cloud level.

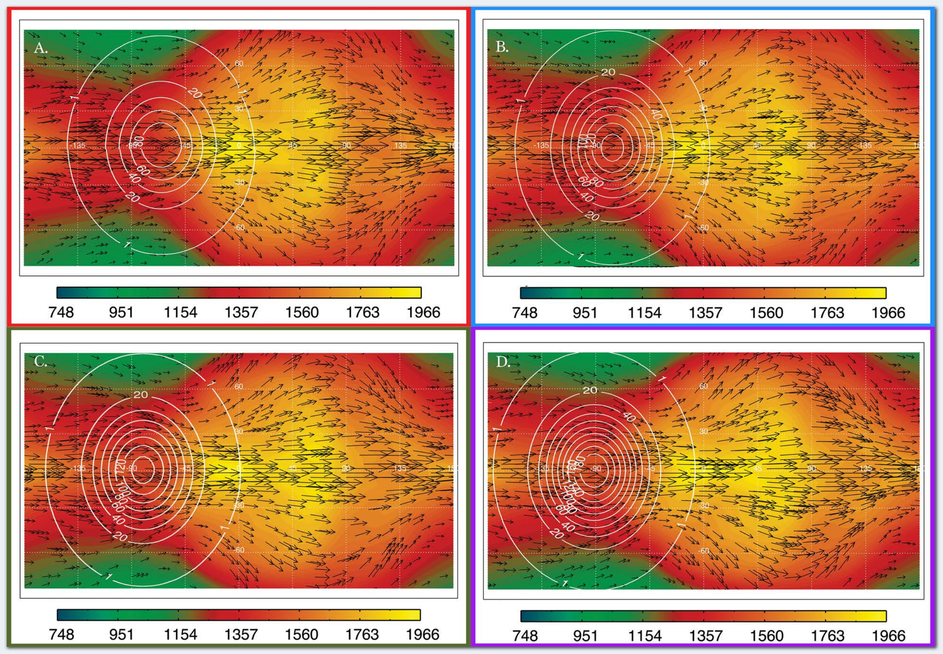

(Right) The predicted IR phase curves express these subtle temperature differences.

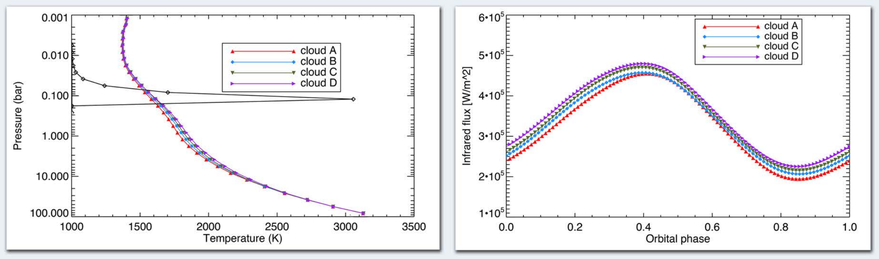

5. Future Work:

We plan run models using different vertical cloud distributions still consistent with the observed visible phase curves. These simulations are our first step in examining the role of prescribed clouds in exoplanet dynamical modeling. Next, we will increase the complexity by including radiative forcing by clouds in the infrared.

References:

Demory, B. O., De Wit, J., Lewis, N., Fortney, J., Zsom, A., Seager, S., ... & Barclay, T. 2013, The Astrophysical Journal Letters, 776(2), L25. "Inference of inhomogeneous clouds in an exoplanet atmosphere"

Muñoz, Antonio García, and Kate G. Isaak. "Probing exoplanet clouds with optical phase curves." Proceedings of the National Academy of Sciences 112.44 (2015): 13461-13466.

Rauscher, Emily, and Kristen Menou. "A general circulation model for gaseous exoplanets with double-gray radiative transfer." The Astrophysical Journal 750.2 (2012): 96.

Toon, O. B., McKay, C. P., Ackerman, T. P., & Santhanam, K. 1989, Journal of Geophysical Research: Atmospheres, 94(D13), 16287-16301. "Rapid calculation of radiative heating rates and photodissociation rates in inhomogeneous multiple scattering atmospheres"